



Contents lists available at <http://www.jmsse.org/> & <http://www.jmsse.in/>

Journal of Materials Science and Surface Engineering



## Phenol Adsorption on Graphite-Hydroxyapatite Nanocomposites: Kinetic and Isotherm Study

Vijaykiran N. Narwade<sup>1,2</sup>, Vanja Kokol<sup>2</sup>, Rajendra S. Khairnar<sup>1</sup>

<sup>1</sup>School of Physical Sciences, Swami Ramanand Teerth Marathwada University, Nanded-431606, Maharashtra, India.

<sup>2</sup>University of Maribor, Faculty of Mechanical Engineering, Institute for Engineering Materials and Design, Smetanova ul. 17, SI-2000 Maribor, Slovenia.

### Article history

Received: 04-Feb-2017

Revised: 22-Feb-2017

Available online: 20-Mar-2017

### Keywords:

Graphite,  
Hydroxyapatite,  
Phenol,  
Adsorption,  
Isotherm,  
Kinetic models

### Abstract

Graphite-Hydroxyapatite (GraHAp) nano-composite is synthesized by wet precipitation method. The synthesized nanocomposite is utilized for adsorption of phenol from aqueous solution, in batch mode experiment. The XRD, FTIR, SEM and EDS characterization techniques are adopted for investigating the crystal structure, functional groups evaluation, surface morphology and elemental analysis of the adsorbent. The XRD analysis confirms the formation of the GraHAp composite. SEM and EDAX spectroscopy reveals the porous nature and presence of elements in the samples. The sorption process is optimized by various influencing factors viz., initial phenol concentration, contact time, GraHAp adsorbent dosage, and pH of the solution. The equilibrium data is fitted to Freundlich and Langmuir isotherms. Both models seem to be valid with the sorption of phenol with GraHAp nanocomposites. The kinetic data is evaluated by first and pseudo second order kinetic models. Pseudo-second order kinetic model is best fitted to kinetic data of phenol adsorption.

© 2017 Science IN. All rights reserved

### Introduction

The recent development of industries causes the emergence of various contaminants which has hostile effects on environment [1]. Phenols and its derivatives are considered as priority pollutants since they are harmful to organisms at low concentrations and many of them have been classified as hazardous pollutants because of their potential harm to human health [2]. Phenolic compounds are common contaminants in wastewaters, being generated from petroleum and petrochemical [3,4], coal conversion, and phenol-producing industries [5]. Phenols are widely used in production of a wide variety of resins including phenolic resins, which are used as construction materials for automobiles and appliances, epoxy resins and adhesives, and polyamide for various applications. Due to the solubility of phenol in water, its presence in water reservoirs is noticed as bad taste and odour. The Environmental Protection Agency (EPA) calls for lowering the phenol content in wastewater to less than  $1 \text{ mg L}^{-1}$  [6]. Inhalation and dermal exposures to phenol for humans are highly irritating to skin, eyes, and could cause malfunction in liver, kidney, and pancreas in human bodies [7-8]. Thus, eradication and complete removal of phenol from waste water by the suitable adsorbents is essential.

Hydroxyapatite, a well-known biomaterial, having the chemical formula as  $\text{Ca}_{10}(\text{PO}_4)_6(\text{OH})_2$ , has chemical resemblance with human bone [9]. HAp has various meritorious properties which leads to its applicability in different fields like biomaterials [10], catalyst [11], gas sensors [12], water treatment [13], etc. It can accept a series of anionic and cationic substitution in its structure due to which it is a remarkable substrate for removal of heavy metals from contaminated soil and water. Hydroxyapatite and its other forms like magnetic hydroxyapatite are used previously for adsorption of phenol. Phenol adsorption is also reported by using

other materials such as bentonite [14], montmorillonite [15], zeolite [16], activated carbon [17]. Composites of graphite-chitosan and graphite hydroxyapatite are also reported for eradication of lead particles from waste water [18-19].

In the present study, Hydroxyapatite as the matrix material and graphite as doping material are used for the synthesis of graphite hydroxyapatite (GraHAp) nanocomposites and it is revealed that this nanocomposites proved to be nanomaterial for efficient phenol adsorption. The doping of graphite in Hydroxyapatite supports  $\pi$ - $\pi$  interaction between phenol rings and graphite sheets causing effective increase in adsorption process.

### Experimental

#### Materials used

Diammonium hydrogen phosphate ( $(\text{NH}_4)_2\text{HPO}_4$  Sigma Aldrich, purity 99.00 %, calcium nitrate tetra hydrate ( $\text{Ca}(\text{NO}_3)_2 \cdot 4\text{H}_2\text{O}$  Sigma Aldrich, Purity 99.00 %), graphite powder (Merck millipore), phenol ( $\text{C}_6\text{H}_5\text{OH}$  Sigma Aldrich, Purity: 99.99%), ammonia solution 25 % ( $\text{NH}_4\text{OH}$  Merck millipore), hydrochloric acid (HCl Merck millipore), sodium hydroxide (NaOH Merck millipore), etc.

#### Procedure for synthesis GraHAp

The synthesis of graphite hydroxyapatite (GraHAp) is carried by wet precipitation method, for which calcium nitrate and diammonium hydrogen phosphate are mixed in such a manner that the stoichiometric ratio of Ca/P should be 1.67 [10]. Initially, the suspension of 5 wt% of graphite is added to the solution of calcium nitrate while stirring. The aqueous solution of diammonium hydrogen phosphate solution is then added to the above mixture at slow rate while maintaining the pH of the

solution between 10-11. The precipitate formed was rinsed with double distilled water until it came to neutrality and dried at 100°C for overnight. The dried sample is grounded using agate mortar and stored for further adsorption study.

### Characterizations

The structural identification of sample was carried out with X-Ray diffraction (XRD). The XRD analysis of synthesized GraHAp is carried out with Rigaku make X-Ray diffractometer (Miniflex) with CuK $\alpha$  ( $\lambda=1.543\text{\AA}$ ) radiation. The thermal stability of material is seen by TG/DTA in the temperature range 40-900 °C. Fourier Transform Infrared (FTIR) study is performed using Perkin Elmer spectrum-1 FTIR model. FTIR spectra are recorded in the range of 400-4000  $\text{cm}^{-1}$ . Scanning electron microscope SUPRA 35 VP (Zeiss, Germany), equipped with energy dispersive X-Ray spectrometry (EDXS), Oxford INCA 350 (Oxford, UK) used for the evaluation of morphology and elemental analysis of adsorbents. The Dynamic Light Scattering (DLS) technique is used to measure particle size of GraHAp composite, by means of NanoBrook 173 Plus Particle Size Analyzer.

### Adsorption study

The solutions of different desired concentrations are prepared via successive dilution of the stock solution of phenol of 1000  $\text{mgL}^{-1}$ . For studying adsorption phenomena, 50 ml of the solution of desired concentration is taken into 100 ml. flasks and added with different weighted adsorbent. The experiments are carried out at room temperature. During adsorption process, speed of shaker is fixed at 160 rpm. The phenol concentration is determined by UV-Vis spectrometer at wavelength 270 nm [20].

The % removal of phenol from solution is carried out using formula [21]

$$\% \text{ removal} = \frac{C_0 - C_e}{C_0} \times 100 \quad (1)$$

The phenol adsorption capacity  $q_e$  ( $\text{mg.g}^{-1}$ ) of GraHAp nanocomposite is verified using formula [21]

$$q_e = \frac{v}{m} (C_0 - C_e) \quad (2)$$

Where,  $v$  is the volume of solution,  $m$  is the mass of adsorbent (gm),  $C_0$  ( $\text{mg L}^{-1}$ ) is initial concentration of phenol,  $C_e$  ( $\text{mg L}^{-1}$ ) is the final concentration of solution after adsorption.

## Results and Discussion

### Characterization of Adsorbent

#### X-ray diffraction

The XRD image clearly reveals the crystalline formation of GraHAp composite (Fig.1). The characteristics peaks of HAp are at  $2\theta$  angle of 32.41, 33.58, 25.44, 50.25, 47.32, 34.71, 38.57, etc. in confirmation with the reported  $2\theta$  values [1], confirming the hexagonal Hydroxyapatite phase with the lattice parameters, viz.,  $a=9.41\text{\AA}$  and  $c=6.88\text{\AA}$  [22]. In addition to this, peak at  $2\theta$  value of 26.31 indicates the presence of graphite suggesting the crystalline formation of GraHAp composite. The average grain size of GraHAp composites is found to be 43 nm which is calculated using the Debye Scherer formula [23]

$$d = \frac{k\lambda}{\beta \cos\theta} \quad (3)$$

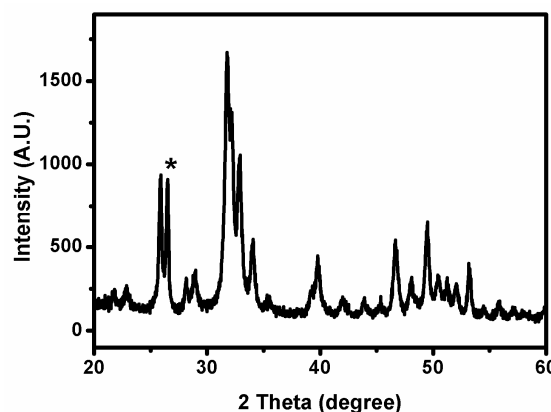


Figure 1: XRD image of GraHAp showing the polycrystalline composite of graphite and Hydroxyapatite compound

#### Fourier transforms infrared spectroscopy

The sample was further investigated by FTIR, and the results are shown in Fig.2. It can be observed that most of the absorbance peaks are well attributed to characteristic peaks of HAp. The FTIR bands at about 966 and 467  $\text{cm}^{-1}$  are ascribed to  $\text{PO}_4^3$  ( $\nu_1$ ) and  $\text{PO}_4^3$  ( $\nu_2$ ), respectively[24]. The bands around 1101  $\text{cm}^{-1}$  and 1031  $\text{cm}^{-1}$  are due to  $\text{PO}_4^3$  ( $\nu_3$ ), and the three adsorption peaks at 637, 604 and 565  $\text{cm}^{-1}$  are assigned to  $\text{PO}_4^3$  ( $\nu_4$ ) [25]. The peaks at 1464, 1395, and 865  $\text{cm}^{-1}$  could be attributed to  $\text{CO}_2$  vibration, which was probably caused by absorption of  $\text{CO}_2$  from atmosphere during preparation under alkaline conditions [26].

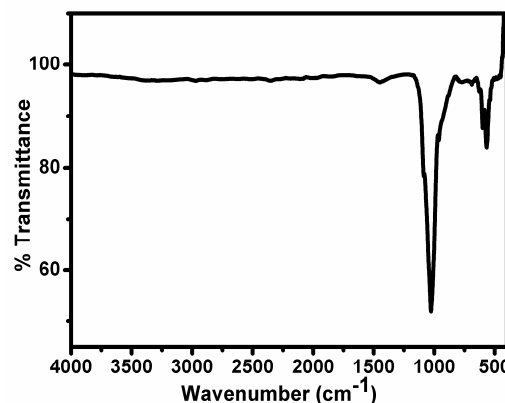


Figure 2: FTIR image of GraHAp composite; important functional groups are described in the text

#### Thermo-gravimetric analysis

TG-DTA profile of GraHAp sample is shown in Fig.3, wherein gradual change in the mass is occurred in the material as a function of temperature. The total weight loss is found to be 11.59%. The weight loss in the region up to 290 °C corresponds to the dehydration of the precipitating complex and also to the loss of physically adsorbed water molecules of the GraHAp powder. The weight loss in this region is 5.78%. The weight loss occurring at higher temperature up to 700 °C is due to evolution of carbon dioxide due to carbonates. The graphite is rather thermally stable, and shows no effect during the thermal treatment [27].

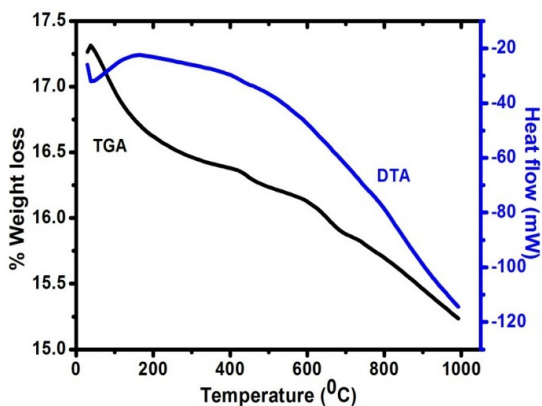


Figure 3: TG/DTA profile of GraHAp composite

SEM and EDS analysis

The scanning electron microscopy images of the GraHAp composite are shown at two magnifications of 5µm and 1 µm (Fig. 4a & 4b). Along with this diagram, 3D surface construction of composite is displayed by means of Image J-software. The particles have varying dimensions (length x breadth) with irregular in height, and having upwards growth. Moreover, the particle arrangement in composites leads to the formation of more pores and cages structures throughout the composite. This kind of morphology on the surface exhibits enormous number of sites, useful for phenol adsorption. This leads to GraHAp substrate as an efficient adsorbent as it is providing more adsorption sites for residing more phenol molecules on surface as well as within the pore in the bulk of GraHAp structure. The average particle size is calculated and is found to be 1.1µm. This particle size distribution as seen by DLS plot shows the average particle size to be of 1µm (Fig 4 d). The EDS image of GraHAp reveals the emergence of various elemental peaks, as expected, with Ca/P ratio of 1.67, confirming the formation of HAP hexagonal phase.

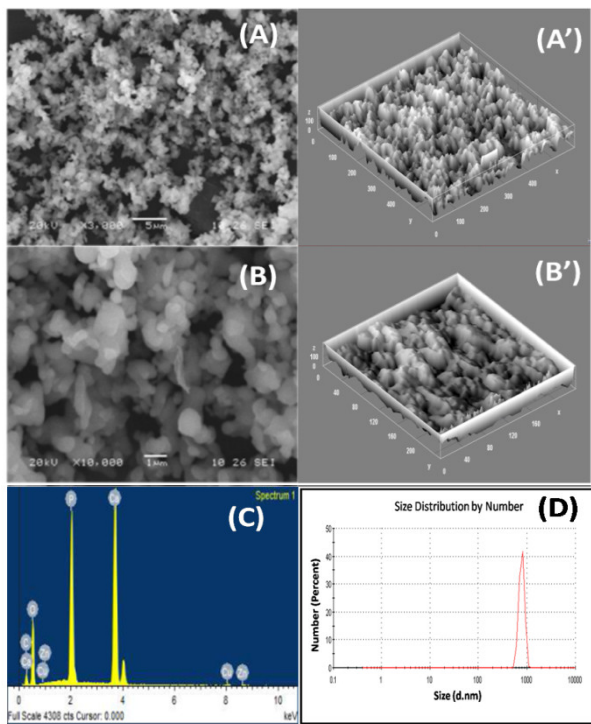


Figure 4: (A) and (B) SEM images (C) EDAX image and (D) DLS spectra of GraHAp

Effect of dose

The dose dependant adsorption of phenol is studied, wherein, different amount of GraHAp composite material, ranging from 0.1 gm to 2 gm, is added to the solution of phenol. Figure 5 shows the effect of GraHAp doses for phenol removal out of initial phenol concentration of 100 mg L<sup>-1</sup>. As the adsorbent dose is going to increase, the phenol removal (%) goes on increasing from aqueous solution. The dose of 2 gm GraHAp gives nearly 79.46% phenol removal, indicating highest removal capacity for the phenol concentration of 100 mg L<sup>-1</sup> with its own pH level.

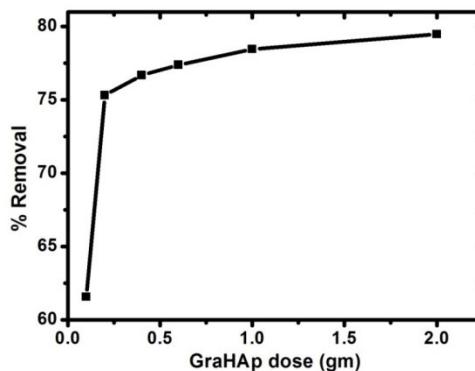


Figure 5: The phenol removal by varying GraHAp dose dissolved in 100 mg L<sup>-1</sup> phenol containing solution

Effect of pH

The Fig. 6 displays the effect of pH for the removal of phenol from solution having variable pH, for a known quantity of dose. At lower pH, there is more removal of phenol from aqueous solution. This may be due to the fact that, the GraHAp composite particles, at lower pH, are surrounded by more positive charges which cause the electrostatic force between phenoxide ions [28]. As the pH of the solution increases, the phenol removal from solution is decreased. Thus, it is observed that maximum of 82.6 % of phenol is removed from aqueous solution having 2pH.

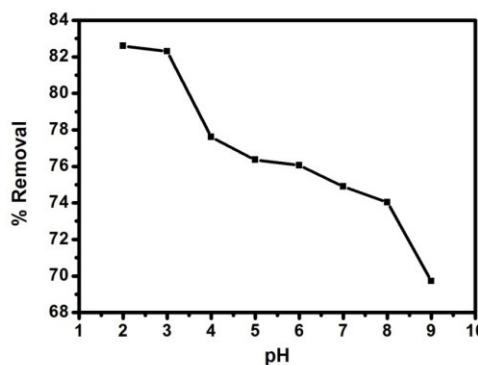
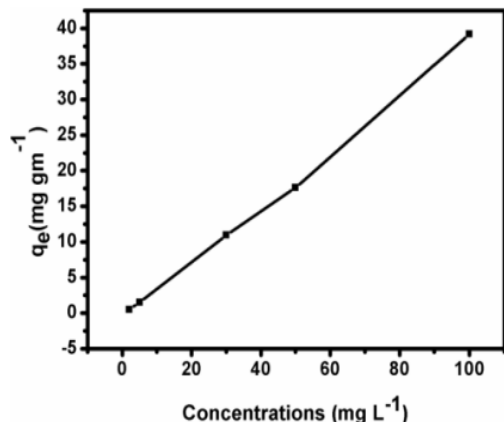


Figure 6: The graph shows the strong dependence of solution pH on the removal of phenol contained in it

Effect of initial concentration

Various solutions of phenol with its concentrations, viz., 2, 5, 15, 30, and 100 mg L<sup>-1</sup> are prepared for this study. The fixed amount of GraHAp added to these solutions and later on kept for shaking for fixed amount of time. After particular fixed time interval, concentration of solution is checked intermittently by means of UV spectroscopy. The value of q<sub>e</sub> is obtained using the equation (2) as described earlier. The Fig. 7 below shows the increment in the q<sub>e</sub> value with initial concentrations of solutions. If

the concentration of phenol is more in the starting solution, the  $q_e$  value of the adsorbent is increased.



**Figure 7:** Effect of initial phenol concentration on its adsorption for a fixed amount of dose and contact time

### Adsorption isotherm

Langmuir and Freundlich isotherm models are used to set up the adsorption equilibrium data. Generally, it is observed that Langmuir isotherm model is supposed to be good for monolayer adsorption while Freundlich isotherm model is useful or heterogeneous surface sites.

The linearized equation for Langmuir isotherm is [29]-

$$\frac{1}{q_e} = \frac{1}{q_0} + \frac{1}{bq_0} \left( \frac{1}{c_e} \right) \quad (4)$$

Where,  $q_e$  is the equilibrium phenol concentration on the adsorbent ( $\text{mg.g}^{-1}$ ),  $q_0$  is the monolayer sorption capacity of the HAP adsorbent ( $\text{mg.gm}^{-1}$ ), and  $C_e$  is the equilibrium phenol concentration in the solution ( $\text{mg.L}^{-1}$ ). The parameter "b" is the Langmuir constant ( $\text{L.mg}^{-1}$ ). The linearized Freundlich isotherm equation is given by [29]

$$\log q_e = \frac{1}{n} \log c_e + \log k_f \quad (5)$$

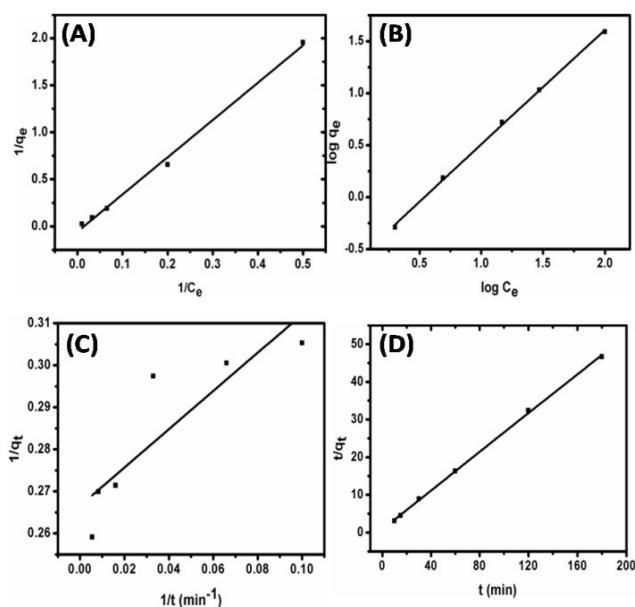


**Figure 8:** Graphical representation of (A) Langmuir isotherm (B) Freundlich isotherm (C) First order kinetic model (D) Pseudo second order kinetic model

Where,  $q_e$  is the equilibrium phenol concentration on the adsorbent ( $\text{mg.gm}^{-1}$ ),  $k_f$  is the empirical constant of Freundlich isotherm ( $\text{L.mg}^{-1}$ ) and  $C_e$  is the equilibrium concentration of the phenol in solution ( $\text{mg.L}^{-1}$ ). The constant  $n$  is the empirical parameter related to the intensity of adsorption, which varies with the heterogeneity of the material. When  $1/n$  values are in the range  $0.1 < 1/n < 1$ , the adsorption process is favorable [31]. Figure 8 (A and B) shows the plots of Langmuir and Freundlich isotherm as determined by above equations. Table 1 displays the isotherm parameters showing both the isotherms are well suited for phenol adsorption on GraHAP as seen from their  $R^2$  values.

**Table 1:** Calculated Parameters of isotherm models

Isotherm	Langmuir			Freundlich		
Parameters	$q_0$	$b$	$R^2$	$k_f$	$n$	$R^2$
Values	17.54	0.0143	0.99	0.254	1.1	0.99

### Kinetic models

The kinetic data obtained is modelled in the form of first-order and pseudo second order kinetic models. The kinetic model depicts the rate of adsorption. The first order kinetic model is given by [28]

$$\frac{1}{q_t} = \frac{k_1}{q_1} \frac{1}{t} + \frac{1}{q_1} \quad (6)$$

Where,  $q_t$  ( $\text{mg.gm}^{-1}$ ) is the adsorption capacity of GraHAP adsorbent at time  $t$ ,  $q_1$  ( $\text{mg.g}^{-1}$ ) is maximum adsorption capacity at equilibrium,  $k_1$  ( $\text{min}^{-1}$ ) is rate constant of the first order kinetic model.

The pseudo second order kinetic model equation is [30]

$$\frac{t}{q_t} = \frac{1}{k_2 q_2^2} + \frac{t}{q_2} \quad (7)$$

Where,  $k_2$  ( $\text{mg.gm}^{-1} \text{min}^{-1}$ ) is the rate constant of pseudo second order kinetic model,  $q_2$  ( $\text{mg.g}^{-1}$ ) is the maximum adsorption capacity at equilibrium of composite. The Fig. 8 (C and D) displays first and second order kinetic models. As per Table 2, pseudo second order kinetic model is valid for phenolic adsorption on GraHAP matrix, as supported by  $R^2$  values.

**Table 2:** Calculated Parameters of Kinetic models

Kinetic model	First order			Second order		
Parameters	$q_1$	$k_1$	$R^2$	$q_2$	$k_2$	$R^2$
Values	3.84	1.728	0.72	4	13.44	0.99

### Conclusions

GraHAP composite is synthesized by wet chemical precipitation method and its functional groups are evaluated by FTIR. XRD revealed the polycrystalline GraHAP composite formation. GraHAP is thermally stable showing minimum weight loss as seen by TGA/DTA. The high value for weight loss in TGA is attributed to highly porous nature of GraHAP compound due to addition of graphite. The porous nature of GraHAP composite adsorbent is confirmed by SEM. These characterisation shows that GraHAP composite is efficient adsorbent material.

The maximum adsorption capacity of GraHAP composite is calculated by Langmuir isotherm and it is found to be  $17.54 \text{ mg.gm}^{-1}$ . The pseudo second order kinetic model is best fitted for phenol adsorption process on GraHAP.

### References

- V.N. Narwade, M. P. Mahabole, K.A. Bogle, and R. S. Khaimar. "Waste water treatment by nanoceramics: Removal of Lead particles." *International Journal of Engineering Science and Innovative Technology (Ijesit)* 3, no. 3, (2014) 324-329.

2. A.Maleki, A. H. Mahvi, R. Ebrahimi, and J. Khan. "Evaluation of barley straw and its ash in removal of phenol from aqueous system." *World Applied Sciences Journal* 8, no. 3, (2010)369-373.
3. J.Michałowicz, and W. Duda. "Phenols—sources and toxicity." *Polish Journal of Environmental Studies* 16, no. 3, (2007) 347-362.
4. G.S.Veeresh, P. Kumar, and I. Mehrotra. "Treatment of phenol and cresols in upflow anaerobic sludge blanket (UASB) process: a review." *Water research* 39, no. 1, (2005) 154-170.
5. R.J. Schmidt,"Industrial catalytic processes—phenol production." *Applied Catalysis A: General* 280, no. 1, (2005)89-103.
6. O. Abdelwahab, N. K. Amin, and ES Z. El-Ashtoukhy. "Electrochemical removal of phenol from oil refinery wastewater." *Journal of hazardous materials* 163, no. 2, (2009) 711-716.
7. A.Ali, and K. Saeed. "Phenol removal from aqueous medium using chemically modified banana peels as low-cost adsorbent." *Desalination and Water Treatment* 57, no. 24, (2016) 11242-11254.
8. G.Busca, S. Berardinelli, C. Resini, and L. Arrighi. "Technologies for the removal of phenol from fluid streams: a short review of recent developments." *Journal of Hazardous Materials* 160, no. 2, 265-288(2008).
9. A.Sobczak, A. Kida, Z. Kowalski, and Z. Wzorek. "Evaluation of the biomedical properties of hydroxyapatite obtained from bone waste." *Polish Journal of Chemical Technology* 11, no. 1, (2009) 37-43.
10. P.N.Chavan, M. M. Bahir, R. U. Mene, M. P. Mahabole, and R. S. Khairnar. "Study of nanobiomaterial hydroxyapatite in simulated body fluid: Formation and growth of apatite." *Materials Science and Engineering: B* 168, no. 1, (2010) 224-230.
11. S.Mallouk,K. Bougrin, A. Laghzizil, and R. Benhida. "Microwave-assisted and efficient solvent-free Knoevenagel condensation. A sustainable protocol using porous calcium hydroxyapatite as catalyst." *Molecules* 15, no. 2, (2010) 813-823.
12. R.U.Mene, M. P. Mahabole, K. C. Mohite, and R. S. Khairnar. "Fe doped hydroxyapatite thick films modified via swift heavy ion irradiation for CO and CO<sub>2</sub> gas sensing application." *Journal of Alloys and Compounds* 584, (2014) 487-493.
13. S.Choi, and Y. Jeong. "The removal of heavy metals in aqueous solution by hydroxyapatite/cellulose composite." *Fibers and Polymers* 9, no. 3, (2008) 267-270.
14. F.A.Banat, B. Al-Bashir, S. Al-Asheh, and O. Hayajneh. "Adsorption of phenol by bentonite." *Environmental pollution* 107, no. 3, (2000) 391-398.
15. Yu, Jae-Young, Mi-Young Shin, Jin-Hwan Noh, and Jung-Ju Seo. "Adsorption of phenol and chlorophenols on Ca-montmorillonite in aqueous solutions." *Geosciences Journal* 8, no. 2 (2004) 185-189.
16. Khalid, Mohamed, Guy Joly, Arlette Renaud, and Patrick Magnoux. "Removal of phenol from water by adsorption using zeolites." *Industrial & engineering chemistry research* 43, no. 17 (2004) 5275-5280.
17. Gundogdu, Ali, Celal Duran, H. Basri Senturk, Mustafa Soylak, Duygu Ozdes, Huseyin Serencam, and Mustafa Imamoglu. "Adsorption of phenol from aqueous solution on a low-cost activated carbon produced from tea industry waste: equilibrium, kinetic, and thermodynamic study." *Journal of Chemical & Engineering Data* 57, no. 10 (2012) 2733-2743.
18. Gedam, Asha H., Rajendra S. Dongre, and Amit K. Bansiwai. "Synthesis and characterization of graphite doped chitosan composite for batch adsorption of lead (II) ions from aqueous solution." *Advanced Materials Letters* 6, no. 1 (2015) 59-67.
19. Zhu, Jiangtao, Hoi Man Wong, Kelvin Wai Kwok Yeung, and Sie Chin Tjong. "Spark plasma sintered hydroxyapatite/graphite nanosheet and hydroxyapatite/multiwalled carbon nanotube composites: mechanical and in vitro cellular properties." *Advanced Engineering Materials* 13, no. 4 (2011) 336-341.
20. Tancredi, Nestor, Natalia Medero, Fabiana Möller, Javier Piriz, Carina Plada, and Tomás Cordero. "Phenol adsorption onto powdered and granular activated carbon, prepared from Eucalyptus wood." *Journal of colloid and interface science* 279, no. 2 (2004) 357-363.
21. J.Nastaj, A. Przewlocka, and M. Rajkowska-Myśliwiec. "Biosorption of Ni (II), Pb (II) and Zn (II) on calcium alginate beads: equilibrium, kinetic and mechanism studies." *Polish Journal of Chemical Technology* 18, no. 3, (2016) 81-87.
22. M.Mathew, and S. Takagi. "Structures of Biological Minerals in." *Journal of Research of the National Institute of Standards and Technology*106, no. 6 (2001).
23. B.M. Pradeep Kumara , K.H. Shivaprasada , R.S. Raveendrab , R. Hari Krishnac , and B.M. Nagabhushana. " Adsorption of Hazardous Methylene Blue from Aqueous Solution using Combustion Derived CaAl<sub>2</sub>O<sub>4</sub> Nanoparticles." *Journal of Materials Science & Surface Engineering* Vol. 4 (7), (2016) 492-495.
24. Y.Qi, J. Shen, Q. Jiang, B. Jin, J. Chen, and Xia Zhang. "The morphology control of hydroxyapatite microsphere at high pH values by hydrothermal method." *Advanced Powder Technology* 26, no. 4, (2015) 1041-1046.
25. H.Chen,and S. Leng. "Rapid synthesis of hollow nano-structured hydroxyapatite microspheres via microwave transformation method using hollow CaCO<sub>3</sub> precursor microspheres." *Ceramics International* 41, no. 2, (2015) 2209-2213.
26. L. An, W. Li, Y. Xu, D. Zeng, Y. Cheng, and G. Wang. "Controlled additive-free hydrothermal synthesis and characterization of uniform hydroxyapatite nanobelts." *Ceramics International* 42, no. 2, (2016) 3104-3112.
27. D.M. Crumpton, R. A. Laitinen, J. Smieja, and D. A. Cleary. "Thermal Analysis of Carbon Allotropes: An Experiment for Advanced Undergraduates." *J. Chem. Educ* 73, no. 6, (1996) 590.
28. K.Lin,J. Pan, Y. Chen, R. Cheng, and X. Xu. "Study the adsorption of phenol from aqueous solution on hydroxyapatite nanopowders." *Journal of Hazardous Materials* 161, no. 1, (2009) 231-240.
29. Y.S. Ho, "Isotherms for the sorption of lead onto peat: comparison of linear and non-linear methods." *Polish Journal of Environmental Studies* 15, no. 1, (2006) 81-86.
30. E.J. Mohammad, A. J. Lafta, and S. H. Kahdim. "Photocatalytic removal of reactive yellow 145 dye from simulated textile wastewaters over supported (Co, Ni) 3O<sub>4</sub>/Al<sub>2</sub>O<sub>3</sub> co-catalyst." *Polish Journal of Chemical Technology* 18, no. 3, (2016) 1-9.

